J. R. Crandall
W. D. Pilkey
W. Kang
C. R. Bass
Department of Mechanical, Aerospace, and Nuclear Engineering
University of Virginia
Charlottesville, VA 22903

Sensitivity of Occupant Response Subject to Prescribed Corridors for Impact Testing

A technology to study the sensitivity of impact responses to prescribed test conditions is presented. Motor vehicle impacts are used to illustrate the principles of this sensitivity technology. Impact conditions are regulated by specifying either a corridor for the acceleration time history or other test parameters such as velocity change, static crush distance, and pulse duration. By combining a time domain constrained optimization method and a multirigid body dynamics simulator, the upper and lower bounds of occupant responses subject to the regulated corridors were obtained. It was found that these prescribed corridors may be either so wide as to allow extreme variations in occupant response or so narrow that they are physically unrealizable in the laboratory test environment. A new corridor based on specifications for the test parameters of acceleration, velocity, crush distance, and duration for frontal vehicle impacts is given. © *1996 John Wiley & Sons, Inc.*

INTRODUCTION

When a sled system is used to simulate the crash response of a vehicle, the deceleration profile or pulse of the sled is often required to stay between prescribed upper and lower bounds called deceleration corridors. Such deceleration corridors are used to regulate crashworthiness tests for automobiles and their accessories. For example, the International Standard Organization (ISO) prescribes a corridor for wheelchair sled tests in evaluating wheelchairs and their tiedown systems in vehicles (Fig. 1). There are several corridors for child restraint system tests including European, American, Japanese, Australian, and Canadian corridors. Figure 2 shows the European ECE R44, American FMVSS 213, and Japanese JIS D0401 corridors for child seat safety tests. Even with sled decelerations confined within a standard corridor, two distinct sled tests can produce occupant and vehicle component responses with substantial dissimilarities. Response sensitivity analysis, which predicts the variation among different experiments with identical corridors, shows that some of the existing standard corridors allow a wide scatter in occupant responses. It is desirable to place sufficient restrictions on crash test pulses to ensure that crash simulation results from different tests within the same corridor are comparable. To this end, this article provides a methodology for defining the shape of deceleration corridors and for deciding which additional impact parameters should be prescribed in the tests.

One of the tools proposed for use in evaluating

Received December 14, 1995; Accepted June 14, 1996.
Shock and Vibration, Vol. 3, No. 1, pp. 435–450 (1996)

CCC 1070-9622/96/060435-16

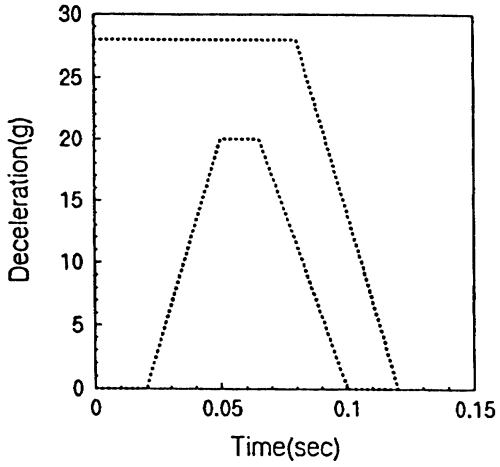

FIGURE 1 ISO wheelchair corridor.

deceleration corridors is a response sensitivity analysis. This analysis uses a game theory, or a constrained optimization method, to find those deceleration profiles that minimize or maximize the peak value of a selected critical response quantity. The deceleration profile that minimizes the peak value of a selected occupant response, such as the chest acceleration of an occupant, is called the *best disturbance*. This minimization is subject to inequality or equality constraints, for example, upper and lower bounds on the deceleration of the sled or the velocity change for the simulated crash. The time history of the occupant response during the impact is called the *best response* if it corresponds to the best disturbance. For example, if the acceleration of the occupant's chest is selected as the critical response whose peak value is minimized when the deceleration profile is $a(t)$, then the chest acceleration calculated from the system model with input $a(t)$ is called the best chest acceleration. Similarly, the sled deceleration curve that maximizes the peak value of a critical response quantity is called the *worst disturbance*. The corresponding time history of the occupant response during the impact is designated the *worst response*.

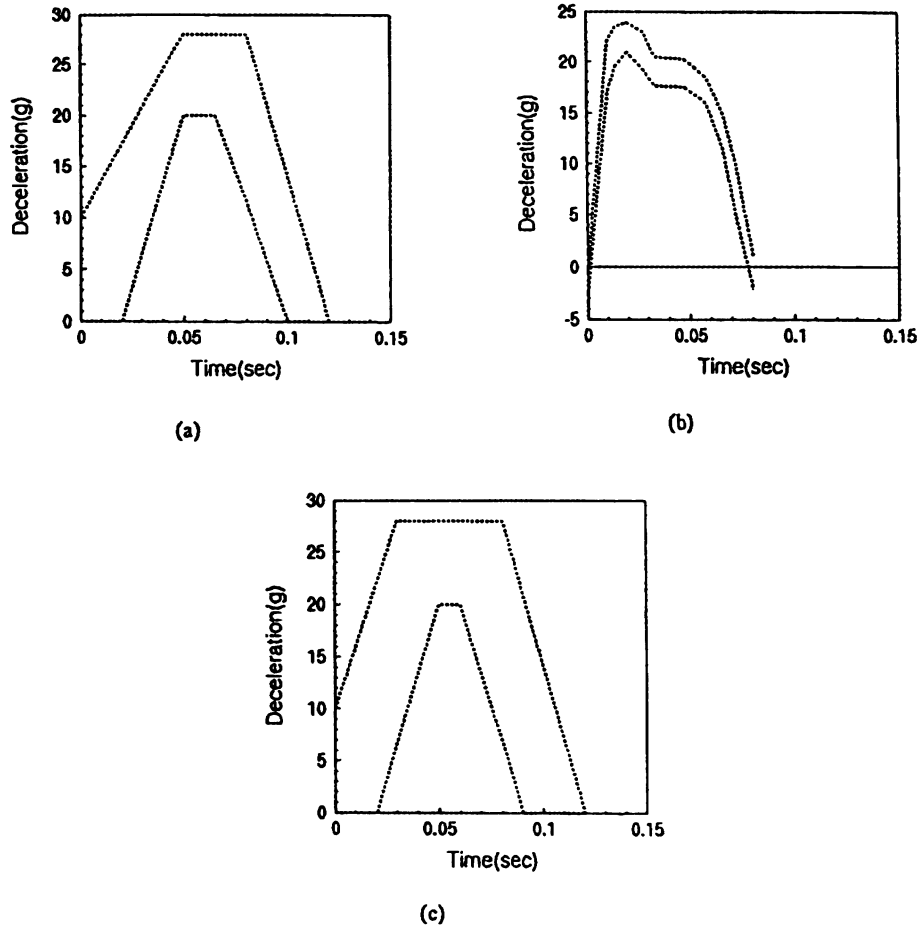

FIGURE 2 Child seat corridors: (a) ECE R44; (b) FMVSS 213; (c) JIS D0401.

The peak values of the critical occupant response parameters for any two tests whose deceleration profiles lie within the same prescribed corridor must fall between the best and worst responses for that corridor. Thus, the best and worst disturbance analysis provides an upper bound of the expected scatter in the occupant response data. A simple and convenient measure of how far apart two test results may be expected to lie is provided by the sensitivity index R, defined as the ratio of the peak occupant response parameter for the worst disturbance to the peak occupant response parameter for the best disturbance.

The best and worst disturbance analysis can be performed using mathematical programming approaches for optimization with inequality and equality constraints. Sevin and Pilkey (1967) formulated this methodology for a single degree of freedom oscillator. Related methods were applied by Sevin and Pilkey (1971) to a variety of shock isolation systems. A formulation that is applicable to the response sensitivity analyses of structures under impact loading was given by Pilkey and colleagues (1993). An outline of this method is given here.

The game theory technique for sensitivity analyses can be used in conjunction with full scale vehicle tests, sled crash tests, and computational simulations. In this study, computer simulations of sled crash tests were used in the sensitivity analysis. The crash analysis results for occupant and restraint systems were obtained using the DYNAMAN occupant simulation package (DYNAMAN, 1991). This program is an enhanced version of the public domain program Articulated Total Body Model (ATB; Fleck and Butler, 1982). ATB has been extensively tested and refined and can, with careful use, provide excellent agreement with laboratory sled tests. In this study, the test conditions included a 3-point belted hybrid III dummy, a 48.3 km/h impact velocity (a velocity change Δv of approximately 53.0 km/h), and a peak sled deceleration of 21 g. Figure 3 depicts the occupant and seat simulation model prior to the crash simulation. Figure 4 shows a comparison between the simulation and sled test of the head and chest resultant accelerations. The level of correlation is good, particularly

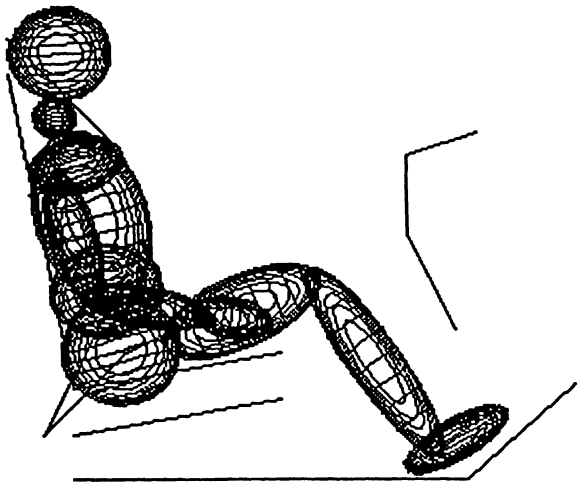

FIGURE 3 Occupant and seat model (ATB).

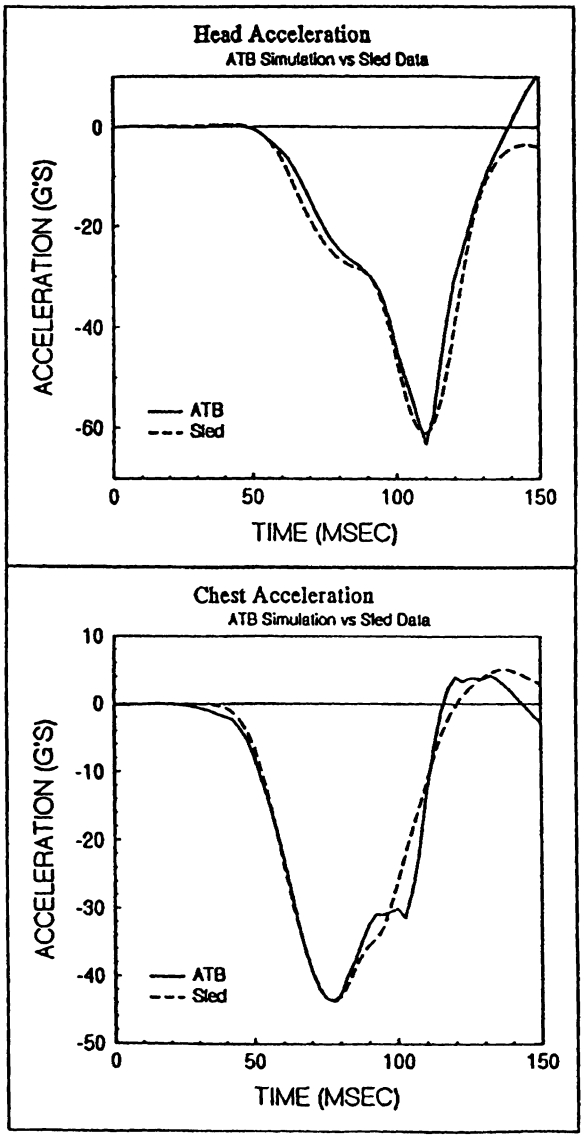

FIGURE 4 Validation of ATB model.

during the critical loading phase, allowing this model to be used with confidence for parameter studies in the vicinity of this baseline.

The best and worst disturbances, or, specifically, the sled deceleration profiles, were obtained by the mathematical programming method proposed here using a simplified occupant and restraint model. The responses of a restrained occupant to these best and worst pulses were then computed using the validated full scale occupant and restraint ATB model. The advantage of this two model combination is that, regardless of how approximate the model used in the mathematical programming may be, the responses of the occupant and restraint system to the best and worst disturbances are obtained from the full scale ATB model.

FORMULATIONS

System Equations

The motion of an occupant and restraint system on a sled or vehicle can be expressed as

$$\ddot{\mathbf{x}} = \mathbf{f}[\dot{\mathbf{x}}, \mathbf{x}, a(t), t] \tag{1}$$

where $\mathbf{x}$ is the state vector of the occupant and restraint system, and $a(t)$ is the sled or vehicle deceleration that is bound by the lower bound $a_L(t)$ and the upper bound $a_U(t)$.

For a linear system, Eq. (1) is usually written as

$$\mathbf{M}\ddot{\mathbf{x}} + \mathbf{C}\dot{\mathbf{x}} + \mathbf{K}\mathbf{x} = \mathbf{M}\mathbf{B}a(t), \tag{2}$$

where $\mathbf{M}$, $\mathbf{C}$, and $\mathbf{K}$ are the mass, damping, and stiffness matrices, respectively. $\mathbf{B}$ is a vector in which the entries corresponding to the horizontal (or the moving direction of the sled or vehicle during frontal impact) displacement of the system are 1 and the rests are zero.

For the best and worst response analysis, a single degree of freedom model was used to represent the occupant and restraint system with the occupant modeled as a mass m and the restraint system as a spring k and damper c. The values of m, k, and c were obtained from the results of a validation effort with sled tests. First, the acceleration, velocity, and displacement responses of the occupant chest to a standard sled deceleration input, e.g., a half-sine pulse, were obtained using the ATB simulation. Then the effective values of m, k, and c were determined using a least squares method in the time domain. The linear model with a sled system is shown in Fig. 5. The absolute displacement of the sled is z and the relative displacement of the mass with respect to the sled is x. The equation governing the motion of the occupant relative to the sled is

$$\ddot{x} + 2\zeta\omega\dot{x} + \omega^2 x = a(t), \tag{3}$$

where $\omega = \sqrt{k/m}$ is the natural frequency of the system, $\zeta = c/(2\sqrt{km})$ is the damping ratio, and $a(t) = -\ddot{z}(t)$ is the deceleration of the sled, also referred to as the deceleration profile or crash pulse. This single degree of freedom system is convenient for predicting trends in the response when the sled deceleration profile and the natural frequency of the occupant and restraint system are varied.

There are two other quantities, velocity change and static crush, associated with a deceleration pulse $a(t)$. They are defined as the following.

Let T denote the duration of the crash pulse and let v_0 be the speed of the sled prior to application of the sled deceleration profile. The velocity change Δv for the sled deceleration $a(t)$ is defined as the difference between the initial speed v_0 and the speed $v(T)$ of the sled at $t = T$,

$$\Delta v = v_0 - v(T) = \int_0^T a(t)\, dt. \tag{4}$$

The static crush distance Δs for a sled with initial speed v_0 and crash pulse $a(t)$ is the distance the sled moves under the action of the deceleration input,

$$\Delta s = \int_0^T v(t)dt = \int_0^T [v_0 - \int_0^t a(\tau)d\tau]dt, \tag{5}$$

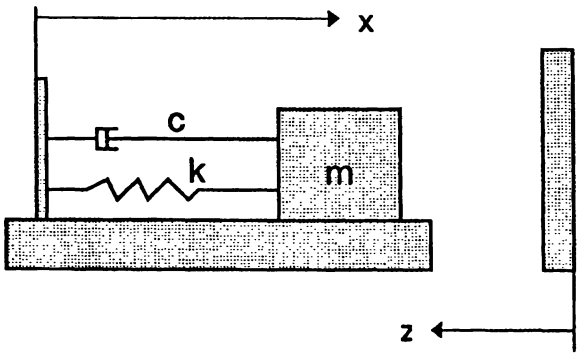

FIGURE 5 Single degree of freedom system.

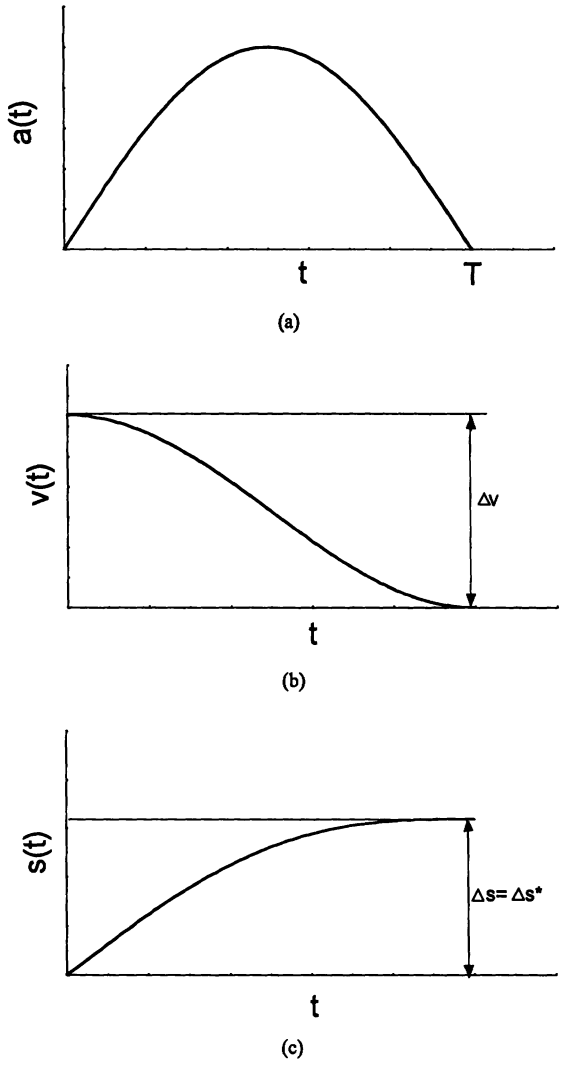

FIGURE 6 Sled motion of an inelastic crash.

which can be expressed in the form

$$\Delta s = (v_0 - \Delta v)T + \int_0^T ta(t)dt. \qquad (6)$$

The collision of vehicles into barriers during frontal impact tests is mainly inelastic due to the deformable front end structure and sheet metal. This motion can be duplicated in a sled test laboratory by use of programmable decelerators to decelerate a test sled. These decelerators are often hydraulic shock absorbers or some deformable materials that are shaped to produce the desired deceleration profile. Figure 6 illustrate typical deceleration, velocity, and displacement time histories for a deceleration sled system.

From Eqs. (1) and (2) it is seen that the motion of the occupant and restraint system relative to a vehicle or sled is determined by the vehicle or sled deceleration pulse $a(t)$. As long as the pulse $a(t)$ is the same, the occupant responses will be identical even though the velocity and displacement of the vehicle or sled are different. Thus, another simulation scheme for sled tests employs the "impulse" or "reverse acceleration" technique. In this scheme, the test sled is initially at rest and is subjected to an acceleration pulse. Figure 7 gives the acceleration, velocity, and displacement of the sled. A third scheme for achieving a sled pulse uses the impact with rebound technique. Here the sled impacts at an initial velocity v_0 and rebounds with a velocity v_T. The deceleration, velocity, and displacement of this type of sled are shown in Fig. 8.

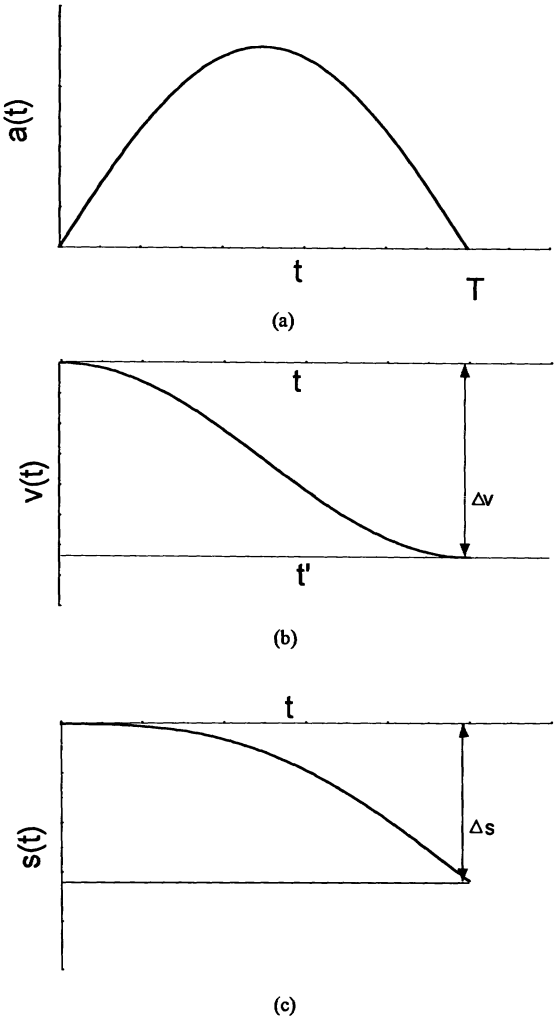

FIGURE 7 Sled motion of an impulse crash.

From these three different sled motions (Figs. 6–8), it is seen that the deceleration pulses $a(t)$ and the velocity changes Δv of the sleds are identical while the displacements are different. To normalize these three kinds of motion, a new value Δs^*, called the *first-order moment of deceleration*, is introduced to regulate the deceleration pulse with the velocity change Δv. Δs^* is defined as

$$\Delta s^* = \int_0^T ta(t)dt. \tag{7}$$

For a motion of a deceleration sled shown in Fig. 6, substitution of $\Delta v = v_0$ into Eq. (6) leads to

$$\Delta s = \Delta s^*. \tag{8}$$

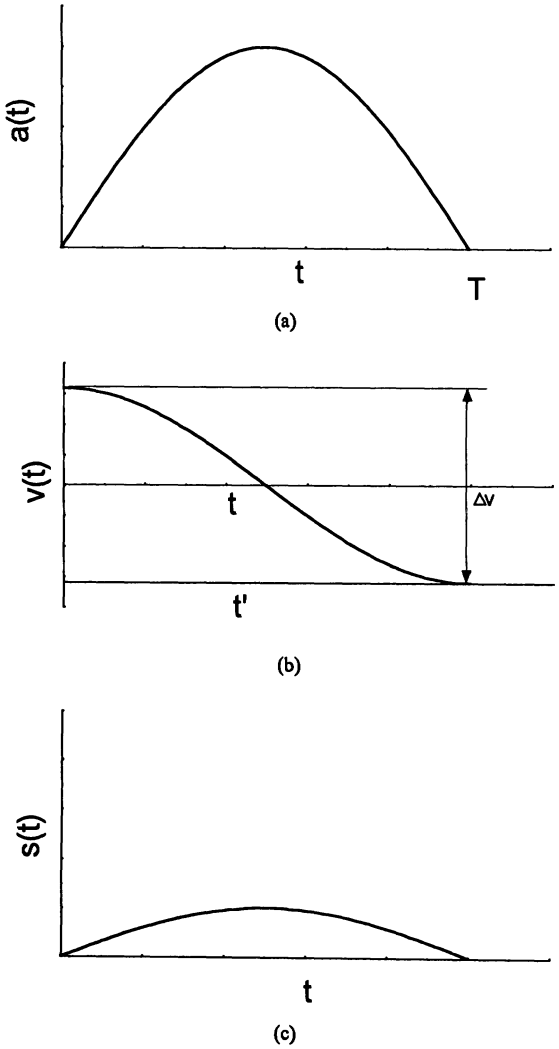

FIGURE 8 Sled motion of an impact with rebound crash.

So, for the perfectly inelastic crash without rebound, the first-order moment of deceleration is equal to the static crush.

For the impulse or reverse acceleration simulation scheme of Fig. 7, if the time axis of the velocity curve of Fig. 7(b) is shifted downward by Δv to t', the velocity in this new coordinate will be

$$v' = \Delta v - \int_0^T ta(t)dt, \tag{9}$$

and the displacement will be

$$\begin{aligned} \Delta s' &= \int_0^T v'dt = \int_0^T \left(\Delta v - \int_0^t a(\tau)d\tau\right) dt \\ &= \Delta vT - \int_0^T \int_0^t a(\tau)d\tau\, dt \\ &= \Delta vT - \left[t \int_0^t a(\tau)d\tau\right]_0^T + \int_0^T ta(t)dt \\ &= \int_0^T ta(t)dt = \Delta s^*. \end{aligned} \tag{10}$$

It can be proved, by shifting the time axis of Fig. 8(b) downward by v_T to t', that the displacement of the impact with rebound sled in this new coordinate is also equal to Δs^*.

Thus, Δs^* can also be considered the *standard static crush*. The standard static crush establishes another measurement for the sled test deceleration pulses that is independent of how the sled pulses are produced. As long as the deceleration time histories of two sled setups are identical, the velocity change and the standard static crush (i.e., the first-order moments of deceleration) are also the same.

The half-sine pulse is often used to represent a typical vehicle deceleration profile and can be expressed as

$$a(t) = A\sin(\pi t/T) \quad 0 \le t \le T, \tag{11}$$

which is shown in Fig. 9. The velocity change is

$$\Delta v = \int_0^T a(t)dt = \frac{2AT}{\pi}, \tag{12}$$

and the standard static crush is

$$\Delta s^* = \int_0^T ta(t)dt = \frac{AT^2}{\pi}. \tag{13}$$

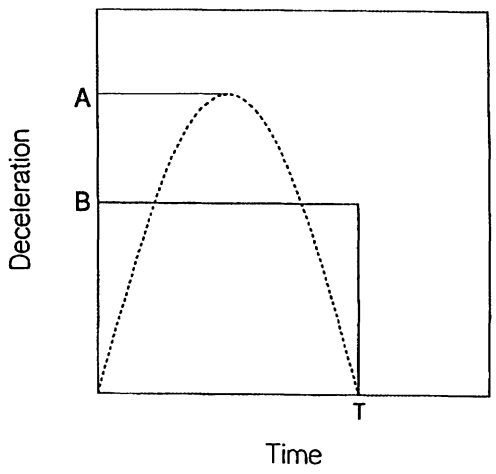

FIGURE 9 Half-sine and rectangular pulses.

Another typical pulse used in sled tests is the rectangle pulse of Fig. 9, defined by

$$a(t) = B \quad 0 \le t \le T. \tag{14}$$

It can be found that when $B = 2A/\pi$, the rectangular pulse will have the same Δv and Δs^* as the half-sine pulse.

Best and Worst Analysis

Suppose the critical response index to predict injury $\Psi(t)$ is selected as a linear combination of the state vector and its derivatives, $\mathbf{x}$, $\dot{\mathbf{x}}$, and $\ddot{\mathbf{x}}$, which is expressed as

$$\Psi(t) = \mathbf{P}\ddot{\mathbf{x}} + \mathbf{Q}\dot{\mathbf{x}} + \mathbf{R}\mathbf{x}, \tag{15}$$

where $\mathbf{P}$, $\mathbf{Q}$, and $\mathbf{R}$ are row vectors.

Equation (15) is a general expression for the selection of any critical response. For example, if the acceleration of the occupant chest is selected as the critical response index, then the first entry of the vector $\mathbf{P}$ is 1 and the remaining entries are 0. Vectors $\mathbf{Q} = \mathbf{R} = \mathbf{0}$.

The goal of the best and worst analysis is to find the sled deceleration profiles that give the extreme occupant responses (i.e., minimum and maximum peak responses) subject to a series of constraints imposed on the sled deceleration profile. This can be expressed as

$$\begin{array}{lll}
\text{find} & a(t) & \text{deceleration pulse,} \\
\text{extremize} & \text{maximum } |\Psi(t)| & \text{response index,} \\
\text{subject to} & \ddot{\mathbf{x}} = \mathbf{f}[\dot{\mathbf{x}}, \mathbf{x}, a(t), t] & \text{system equation,} \\
& a_L(t) \le a(t) \le a_U(t) & \text{deceleration corridor,} \\
& \Delta v_L \le \Delta v \le \Delta v_U & \text{velocity change range,} \\
& \dot{a}_L(t) \le \dot{a}(t) \le \dot{a}_U(t) & \text{deceleration slope range,} \\
& \Delta s_L^* \le \Delta s^* \le \Delta s_U^* & \text{standard static crush constraint,}
\end{array} \tag{16}$$

where $a_L(t)$ and $a_U(t)$ are the lower and upper bounds of the deceleration corridor, Δv_L and Δv_U are the lower and upper bounds for the velocity change, and Δs_L^* and Δs_U^* are the lower and upper bounds for the standard static crush. The term $\dot{a}(t)$ is the derivative of $a(t)$ with respect to time that reflects the rate of change of the deceleration profile. $\dot{a}_L(t)$ and $\dot{a}_U(t)$ are the lower and upper bounds of the slope. Equation (16) can be solved using linear, nonlinear, or dynamic programming algorithms.

EFFECT OF RISE TIME

Most specifications for deceleration corridors contain no restrictions on the rise of the crash pulse. Parametric studies with the single degree of freedom model indicate that rise time has a negligible effect on the crash response if the natural frequency of the occupant and restraint system is sufficiently low relative to the duration of acceleration time history. For an occupant and restraint system with high natural frequency, however, the effect of a decrease in rise time is an increase in the severity of the response. As an example, consider a crash with $\Delta v = 52.6$ km/h and $\Delta s^* = 0.732$ m. If the deceleration time history is represented as a half-sine pulse, Eqs. (12) and (13) provide the duration $T = 0.1$ s and the amplitude $A = 23.42g$ for the half-sine pulse. On the other hand, if the deceleration profile is modeled as a rectangular pulse, the duration T is

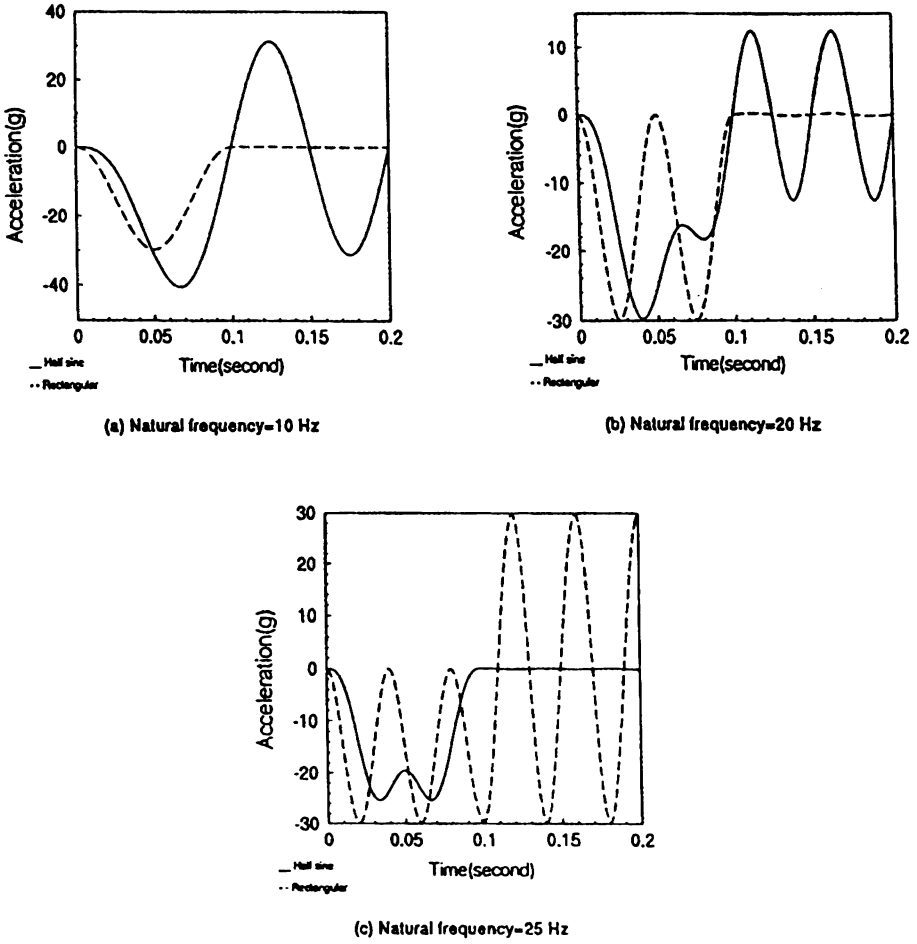

FIGURE 10 Responses of a single degree of freedom system to the pulses of Fig. 9.

still 0.1 s and the amplitude is given by Eq. (14) as $B = 14.91g$. Thus, the amplitude of the rectangular pulse, which has zero rise time, is smaller than that of the half-sine pulse, which has a nonzero rise time.

The acceleration response of a single degree of freedom system subjected to these two deceleration profiles is shown in Fig. 10, where the solid curves are for the half-sine profile and the dashed curves are for the rectangular profile. When the system natural frequency is 10 Hz [Fig. 10(a)], the acceleration response to the half-sine pulse has a higher peak value than the response to the rectangular pulse because of the higher amplitude of the half-sine pulse. When the system natural frequency is increased to 20 Hz [Fig. 10(b)], the two peak values of the acceleration response become almost the same. When the system natural frequency is taken as 25 Hz [Fig. 10(c)], however, the rectangular pulse produces a much higher peak acceleration. This behavior persists at all natural frequencies higher than 25 Hz.

Using the more complete model from the ATB simulation, Fig. 11 shows the response of the occupant and restraint system subject to the half-sine and the rectangular profiles, respectively. These plots depict the resultant acceleration of the dummy chest versus time response with the fundamental natural frequency of the occupant and the safety belt system less than 10 Hz. Similar to the single degree of freedom model with a low natural frequency, the peak acceleration responses, 44.7 and 38.1g, are of similar magnitude, with the half-sine pulse producing a slightly higher peak value.

NECESSITY OF UPPER BOUND

It is sometimes assumed that upper bound curves for deceleration corridors are unnecessary be-

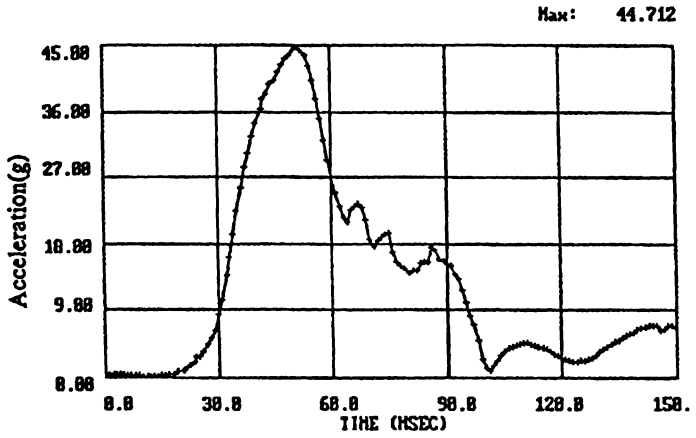

(a) Half sine

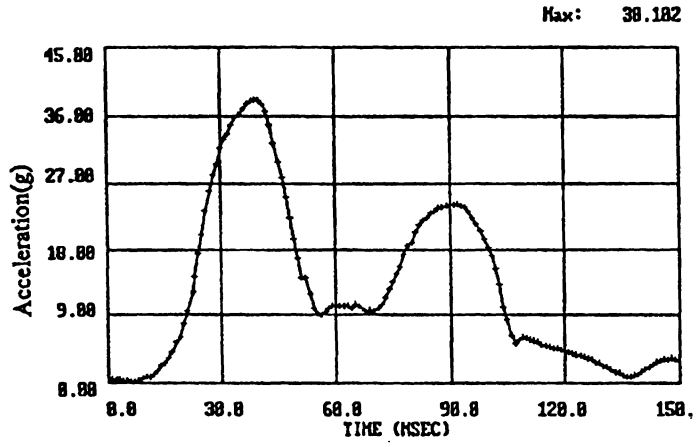

(b) Rectangular

FIGURE 11 Chest accelerations to the pulses of Fig. 9; (a) half-sine; (b) rectangular.

cause it is believed that any deceleration profile lying above a specified lower bound will lead to a more severe response than any pulse at or below that bound. It is shown in this section that this is not always true and that it is generally desirable to have both upper and lower bounds on a deceleration corridor.

Consider the two deceleration profiles shown in Fig. 12. Profile 1 begins as a straight line through the origin, reaches its peak A, and maintains a constant amplitude A until the end of the impact event. Profile 2 begins with an amplitude αA at $t = 0$, which it maintains until it intersects profile 1, after which the two pulses are coincident. Figure 13 shows the displacement response of a single degree of freedom model under the action of these pulses, the solid curve for profile

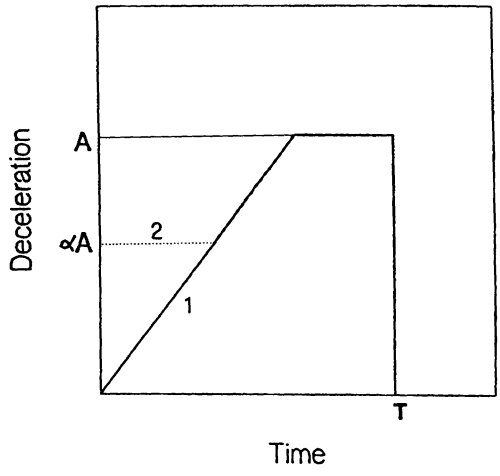

FIGURE 12 Two pulses.

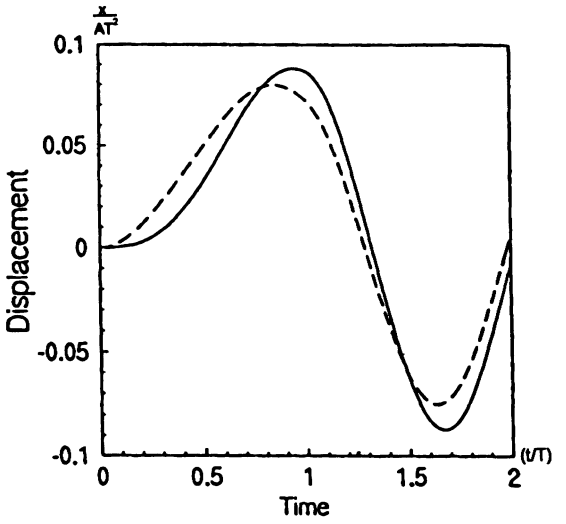

(a) Natural frequency=6 Hz, α=0.58

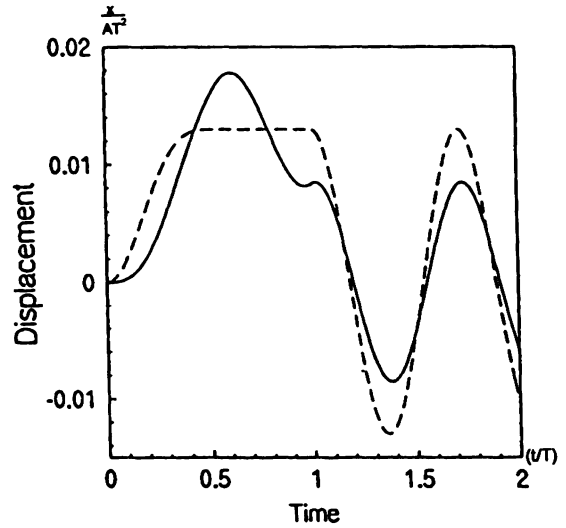

(b) Natural frequency=11.64 Hz, α=0.432

FIGURE 13 Responses of a single degree of freedom system to the pulses of Fig. 12: (a) natural frequency = 6 Hz, α = 0.58; (b) natural frequency = 11.64 Hz, α = 0.432.

1 and the dashed curve for profile 2. The horizontal axis variable in these plots is a normalized time $\tau = t/T$, and the vertical axis variable is a normalized displacement $\eta = x/(AT^2)$. In Fig. 13 the peak displacement for profile 2, which lies above profile 1 and has a higher velocity change Δv, is smaller than that for profile 1.

The ATB simulations of the occupant and restraint system show that similar results are observed in the sled or vehicle impact environment.

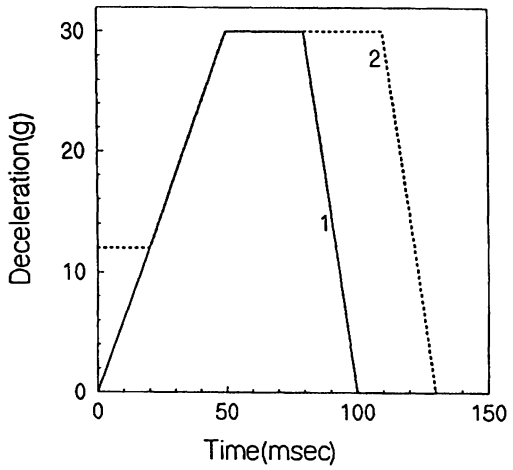

FIGURE 14 Two pulses for ATB simulation.

The applied pulses are shown in Fig. 14 and the occupant chest acceleration responses are depicted in Fig. 15. Again, it is seen that the pulse with the higher amplitude and the longer duration results in a less severe response of the occupant. Therefore, it is necessary to impose both upper and lower bounds when specifying an deceleration corridor.

SENSITIVITY OF DECELERATION BASED CORRIDOR

To ensure that any proposed biomechanics deceleration corridor accurately reflects a full vehicle crash, ten 48 km/h (nominal initial velocity) barrier tests of late model cars were selected from the National Highway Traffic Safety Administration (NHTSA) vehicle data base. The signals were processed with a 60 Hz (−3 db cutoff) filter and an average acceleration time history for the 10 vehicles was computed. This acceleration time history is graphically displayed with an $a(t) \pm 1$ standard deviation envelope (Fig. 16). The upper and lower bounds of this envelope were chosen as the outer limits of an deceleration corridor, and a sensitivity analysis of the occupant's chest acceleration response was performed for this corridor. The best and worst pulses are shown in Fig. 16. Because there are no restraints on the velocity change Δv and the standard static crush Δs^* for this corridor, the last three constraints in Eq. (16) are not included in this sensitivity analysis. The occupancy accelerations associated with the best and worst sled deceleration pulses were calculated using the ATB simulation (Fig. 17).

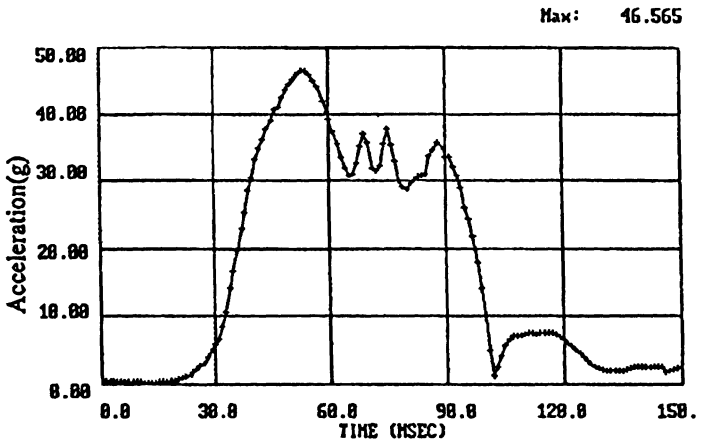

(a) With pulse 1

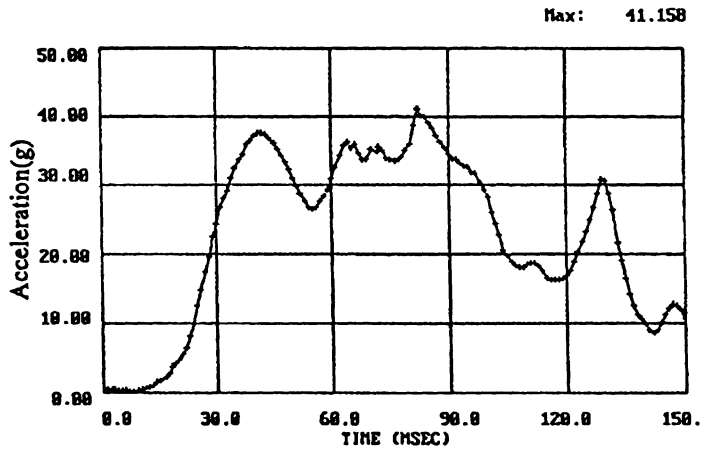

(b) With pulse 2

FIGURE 15 Chest accelerations to the two pulses of Fig. 14: (a) with pulse 1; (b) with pulse 2.

The sensitivity index R, which is taken as the ratio of the worst peak chest acceleration to the best, is

$$R = 58.1g/30.0g = 1.94. \tag{17}$$

Thus, the peak value of the worst response is nearly twice that of the best response. This indicates that this corridor is too wide to provide meaningful comparison among sled tests conducted within the corridor. The results suggest that additional constraints must be imposed to "tighten" the corridor.

Similar sensitivity analysis were performed for a variety of prescribed test corridors. Table 1 lists the sensitivity indices of the ISO corridors for wheelchair sled tests, and the European ECE R44, American FMVSS 213, and Japanese JIS D0401 corridors for child seat safety tests. These sensitivity indices were obtained from the best and worst disturbance analyses and the ATB simulations of the full scale occupant and restraint system. For the wheelchair corridors, an ISO surrogate and a 50th percentile hybrid III dummy were used in the analyses. The critical response selected for the computation of the sensitivity index R here was the peak value of the wheelchair tiedown force. For the child seat corridors, a child booster seat and a 6-year-old child dummy were used. The critical response in this case was taken to be the peak value of the force in the child seat restraint belt. It is seen from Table 1 that all but

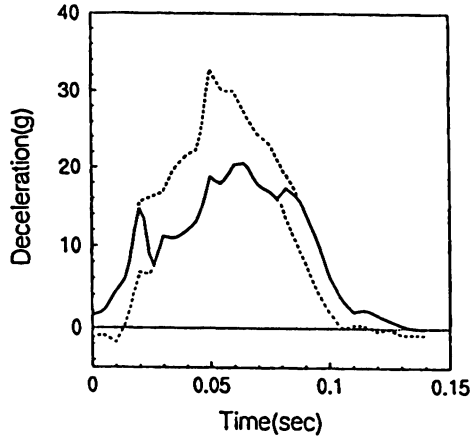

(a) Best pulse

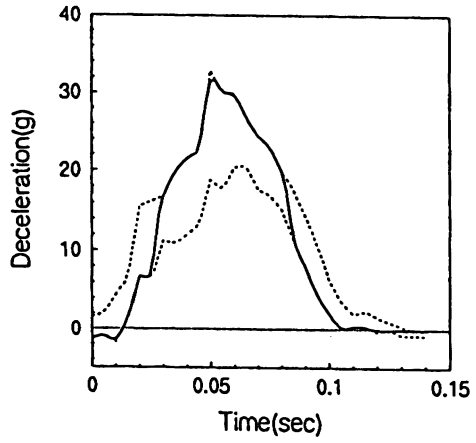

(b) Worst pulse

FIGURE 16 Best and worst pulses via vehicle corridor: (a) best pulse; (b) worst pulse.

one of these corridors allowed a fairly broad scatter in results for different sled tests. The exception, FMVSS 213, gives a sensitivity index of 1.22 for the selected critical response. The complex shape of this corridor, however, may be unnecessarily difficult to achieve with many types of sled systems. It will be shown that a less complex corridor can be developed that would provide the same sensitivity and would be easier to achieve for most sled systems.

Table 1. Sensitivity Indices of Several Corridors

	ISO	ECE R44	FMVSS213	JIS D0401
Sensitivity (R)	1.63	1.35	1.22	1.40

PARAMETRIC CHARACTERIZATION OF DECELERATION TIME HISTORIES

An alternative to narrowing existing deceleration corridors, which may result in a corridor unattainable by some sled systems, is to use additional prescribed parameters to characterize classes of comparable acceleration time histories. In particular, the specification of the velocity change Δv, the standard static crush Δs^*, and the pulse duration T appears sufficient to characterize the impact event. The adequacy of any proposed set of parameters to define classes of acceleration time histories that are to be regarded as comparable is most easily studied by best and worst disturbance analysis. If the corresponding best and worst responses are comparable, the parameters define a group of deceleration profiles that may be expected to produce similar responses. If, on the other hand, the resulting best and worst responses turn out to vary significantly, the chosen set of parameters is not sufficient to represent classes of similar deceleration profiles and additional restrictions or parameters are required.

To test whether the parameters Δv, Δv^*, and T can adequately define crash pulses, the best and worst disturbance analysis was applied to the occupant and restraint system. The critical response index to predict injury was chosen to the chest resultant acceleration. The crash pulse parameters were assigned the following restricted ranges of values: 48.3 km/h $\leq \Delta v \leq$ 49.9 km/h, 0.58 m $\leq \Delta s^* \leq$ 0.64 m, $0 \leq T \leq$ 120 ms. The occupant mass and the stiffness and damping of the restraint system are given by m = 70 kg, k = 220000 N/m, ζ = 0.05 [Eq. (3)].

Using the peak acceleration of the occupant as the critical response, the best and worst pulses (i.e., the sled decelerations for which the performance measure is minimized and maximized), respectively, are shown in Fig. 18. These pulses, determined by the single degree of freedom model, are used as input to the ATB model for the occupant and restraint system. Figure 19 shows the chest acceleration of the occupant dummy corresponding to the best and the worst pulse, respectively. The sensitivity index R in this case is the ratio of the worst peak chest acceleration to the best,

$$R = 81.9g/33.9g = 2.42. \quad (18)$$

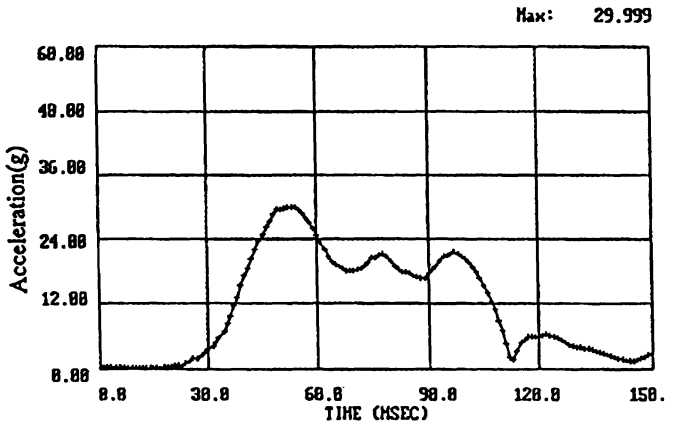

(a) With best pulse

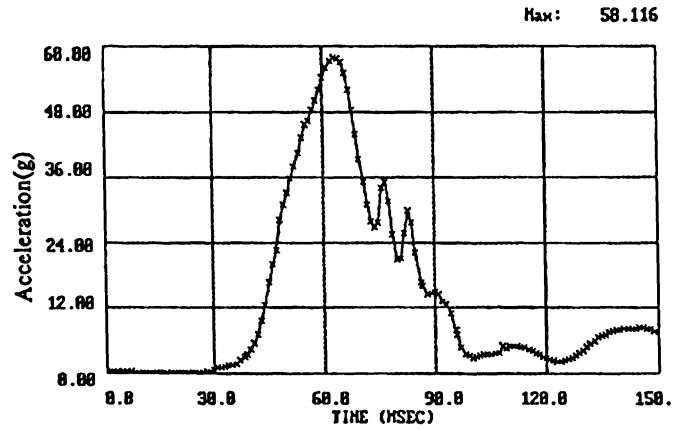

(b) With worst pulse

FIGURE 17 Chest accelerations to the best and worst pulses of Fig. 16: (a) with best pulse; (b) with worst pulse.

Thus, even though both the worst and the best pulse have the same Δv, Δs^*, and T inequality constraints, the peak value of the worst response is 2.42 times that of the best response. In other words, the maximum difference between response data for any two pulses with same Δv, Δs^*, and T constraints is 142%. Although the constraints on the parameters were reasonable, the sensitivity analysis indicates that the set of parameters chosen allows too wide a scatter in the response data.

PROPOSED POTENTIAL CORRIDOR FOR CHEST INJURIES

For restraint system tests and occupant injury criteria tests, half-sine and rectangular accelera-

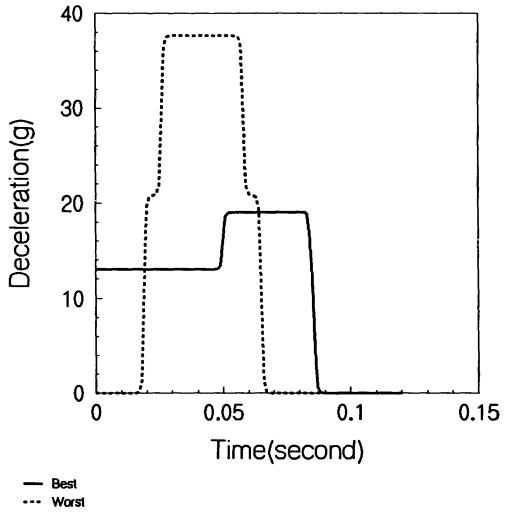

FIGURE 18 Best and worst pulses.

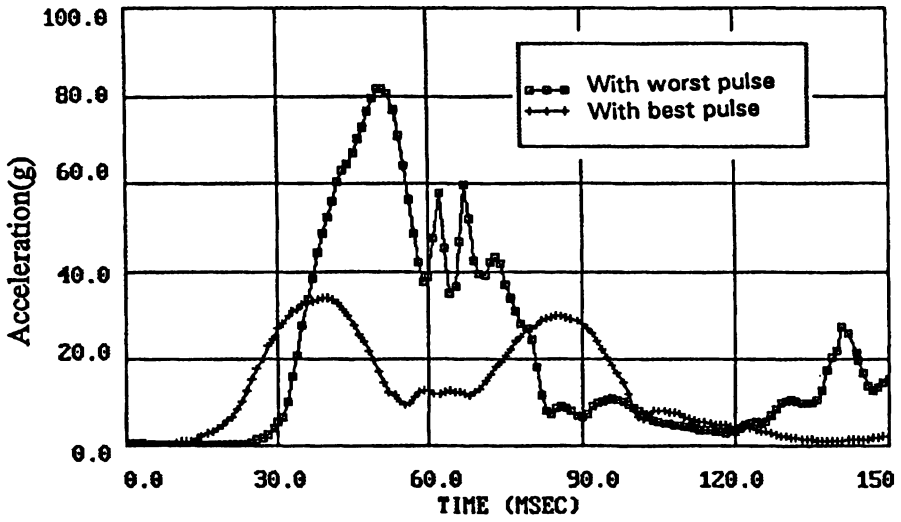

FIGURE 19 Chest accelerations to the best and worst pulses of Fig. 18.

tion time histories were proposed as the basic profile shapes to regulate sled tests in automobile safety laboratories. Sled deceleration profiles lying within a corridor around these shapes may be regarded as equivalent. This section proposes a potential corridor, based on the best and worst disturbance analyses described above, that is applicable to chest acceleration injuries. The choice of this corridor, and of corridors in general, requires a reasonable tightness so that the responses found by different laboratories do not show unacceptable levels of scatter. To ensure this, pulses not only be required to remain within the corridor but should also satisfy parametric constraints, such as those placed on velocity change, standard static crush distance, and so on.

A reasonable corridor can be described by defining pulse duration T, peak amplitude A, velocity change Δv, and standard static crush distance Δs^*. Typical values are as follows

$$\begin{aligned} 48.3\ \text{km/h} \le \Delta v \le 49.9\ \text{km/h}, \\ 0.58\ \text{m} \le \Delta s^* \le 0.64\ \text{m}, \\ 0\ \text{ms} \le T \le 120\ \text{ms}, \\ 0g \le A \le 20g. \end{aligned} \tag{19}$$

Using the single degree of freedom model with its natural frequency equal to the fundamental natural frequency of the occupant and safety belt system, which is 8.9 Hz, the best and worst pulses subject to the corridor defined above were found (Fig. 20). The best pulse produced the minimum peak chest acceleration among all profiles lying in the proposed corridor while the worst pulse corresponded to the maximum peak chest acceleration.

Figure 21 shows the occupant chest accelerations from the ATB simulation under the action of the best and worst pulses. The ratio of the worst to best peak acceleration is

$$R = 48.89g/37.06g = 1.32. \tag{20}$$

So, for different sled pulses lying in this corridor, the chest accelerations can vary by 32%. This variation is less than these of any existing corridor except the FMVSS213. But the

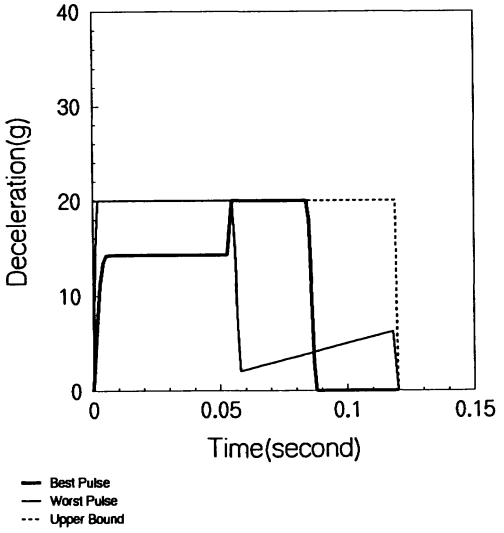

FIGURE 20 Best and worst pulses via proposed corridor.

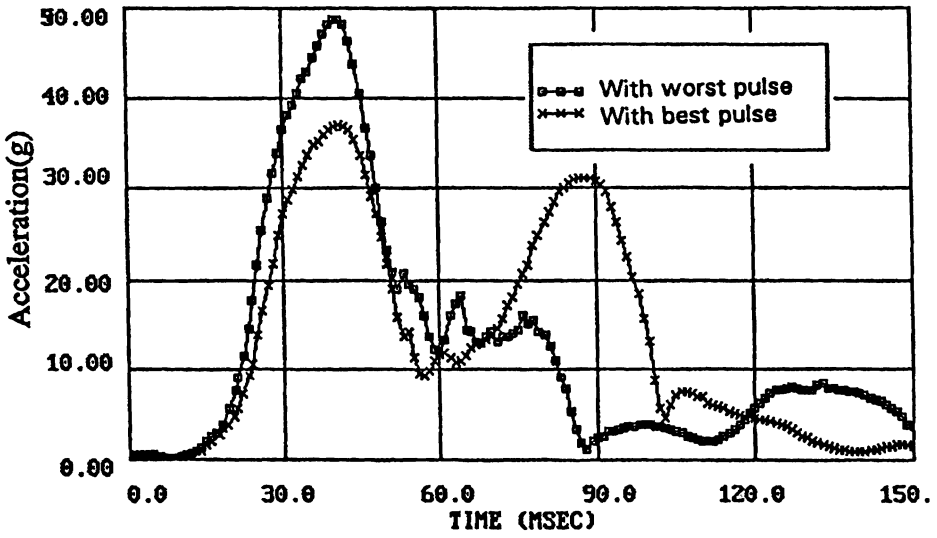

FIGURE 21 Chest accelerations to the best and worst pulses of Fig. 20.

FMVSS213 may involve unnecessary complexity and may be considered too narrow to be followed by many test sled systems. The corridor proposed in Eq. (19) has only upper bounds for the pulse peak and duration time and provides more flexibility on the shape of a deceleration pulse for a particular test sled. The Δv and Δs^* constraints are relatively easy to satisfy for most sled systems. Therefore, this proposed corridor would provide a reasonable "tightness" on the sensitivity of occupant response while still allowing flexibility in sled test systems.

It should be noted that the rise time, although it has an effect on the occupant response as discussed earlier, was not introduced into the proposed corridor. This is because the fundamental natural frequency of the occupant and safety belt system was low enough to allow the effect of rise time to be ignored. For systems with a higher natural frequency, such as a car seat, rise time should be included in the set of parameters characterizing equivalent crash pulses.

CONCLUSIONS

The best and worst disturbance analysis is a useful tool in evaluating the effectiveness of a proposed set of parameters for defining crash pulses that can be considered comparable or equivalent. The best and worse disturbance analysis methodology was applied to the problem of determining practical guidelines for defining deceleration corridors for impact tests. A corridor for chest injuries was proposed that will allow reproduction in different test environments while providing reasonably tight constraints on variation in occupant response among deceleration profiles within the corridor. Analysis of a selected occupant response parameter, chest accleration, to deceleration profiles within this new corridor showed an approximate 32% variation from best response to worst response. In addition to bounds on the test vehicle deceleration, this new corridor includes parametric constraints on velocity change, static crush, and pulse duration.

Other practical guidelines for the selection of test corridors were established. First, the specification of velocity, static crush, and pulse duration was not sufficient to provide an adequately constrained test corridor. Sensitivity of over 140% was shown among test conditions within a selected corridor using only these specifications. Second, to prevent widespread variation in occupant response, it was necessary to include an upper bound on the test system deceleration when establishing deceleration corridors. Substantial variation in occupant responses were shown under test conditions within corridors unbounded from above. Finally, the effect of rise time in system deceleration was negligible if the natural periods of the occupant/restraint system was large compared to the duration of the deceleration.

REFERENCES

DYNAMAN *User's Manual,* 1991, Version 3.0, GESAC Inc., Kearneysville, WV.

Fleck, J. T., and Butler, F. E., 1982, *Validation of the Crash Victim Simulator,* Report Number DOT-HS-806, Vols. I–IV, Calspan Corp. Final Report, Buffalo, NY.

Pilkey, W. D., Kang, W., and Kitis, L., 1993, "Best and Worst Disturbance Analysis of Structures under Crash Pulse Loadings," *Crushworthiness and Occupant Protection in Transportation Systems,* Vol. AMD-169, Vol. BED-25, ASME, New York, pp. 105–113.

Sevin, E., and Pilkey, W. D., 1967, "Computational Approaches to the Min-Max Response of Dynamic Systems with Incompletely Prescribed Input Functions," *Journal of Applied Mechanics,* Vol. 89, pp. 87–90.

Sevin, E., and Pilkey, W. D., 1971, *Optimum Shock and Vibration Isolation,* The Shock and Vibration Information Center, United States Department of Defense, Washington, D.C.